Available online at www.sciencedirect.com

ScienceDirect

Vision Research 46 (2006) 4449–4463

Vision Research

www.elsevier.com/locate/visres

A proposed role for all-*trans* retinal in regulation of rhodopsin regeneration in human rods

A. Navid *, S.C. Nicholas, R.D. Hamer

Smith-Kettlewell Eye Research Institute, 2318 Fillmore St., San Francisco, CA 94115, USA

Received 13 June 2006; received in revised form 25 July 2006

Abstract

In order to account for the multi-phasic dynamics of photopigment regeneration in human rods, we developed a new model of the retinoid cycle. We first examined the relative roles of the classical and channeling mechanisms of metarhodopsin decay in establishing these dynamics. We showed that neither of these mechanisms alone, nor a linear combination of the two, can adequately account for the dynamics of rhodopsin regeneration at all bleach levels. Our new model adds novel inhibitory interactions in the cycle of regeneration of rhodopsin that are consistent with the 3D structure of rhodopsin. Our analyses show that the dynamics of human rod photopigment regeneration can be accounted for by end-product regulation of the channeling mechanism where all-*trans* retinal (*tral*) inhibits the binding of 11-*cis* retinal to the opsin.*tral* complex.

Keywords: Rhodopsin; Retinoid cycle; Computational modeling; Rhodopsin regeneration; End-product regulation

1. Introduction

Light perception in vertebrates' photoreceptors is mediated by G-protein-coupled receptors called opsins. Rhodopsin is the light-sensing molecule of rod photoreceptors. It is composed of the opsin protein and a vitamin A-1 derived chromophore, 11-*cis* retinal (*cral*). The chromophore is attached to the active site of rhodopsin via a Schiff base bond with Lys^{296}. In the dark, a salt bridge between the protonated Schiff base and Glu^{113} stabilizes the ground state conformation of rhodopsin. When a photon interacts with *cral* it causes the chromophore to isomerize to its all-*trans* configuration (*tral*). This isomerization induces a number of intra-molecular steric interactions that lead to disruption of the salt bridge and conversion of rhodopsin into its active form, metarhodopsin II (*MII*) (Bifone, de Groot, & Buda, 1997; Meng & Bourne, 2001; Ritter, Zimmermann, Heck, Hofmann, & Bartl, 2004; Yamada, Yamato, Kakitani, & Yamamoto, 2004). Subsequently *MII* interacts with transducin, a heterotrimeric G-protein that in turn initiates the reactions of the phototransduction cascade (for reviews see Burns & Arshavsky, 2005; Burns & Lamb, 2003; Burns & Taylor, 2001).

Rhodopsin is rapidly deactivated through the action of rhodopsin kinase which phosphorylates a number of serines and threonines on the C-terminal of rhodopsin (Arshavsky, 2002; Kennedy, Lee, Niemi, Craven, & Garwin, 2001; Ohguro, Van Hooser, & Milam, 1995; Zhang, Sports, Osawa, & Weiss, 1997). Final quench of *MII* activity occurs when its transduction interaction site is capped by the water soluble protein, arrestin. Following inactivation, in order to regain photosensitivity, rhodopsin requires the isomerization of *tral* back to *cral* and its re-insertion and attachment to rhodopsin's active site. In vertebrate photoreceptors this process occurs through a collection of chemical reactions known as the retinoid cycle or visual cycle (reviewed in Lamb & Pugh, 2004; McBee, Palczewski, Baehr, & Pepperberg, 2001; Rando, 2001; Saari, 2000).

* Corresponding author.
E-mail address: anavid@ski.org (A. Navid).

0042-6989/$ - see front matter © 2006 Elsevier Ltd. All rights reserved.
doi:10.1016/j.visres.2006.07.035

Reactions of the retinoid cycle take place within the rod outer segment (ROS) and retinal pigment epithelium (RPE) and are depicted in Fig. 1.

The first step of the retinoid cycle involves decay of *MII* which begins with hydrolysis of the Schiff base bond between *tral* and Lys^{296}. Concurrent with this process a storage form of rhodopsin, metarhodopsin III (*MIII*) is generated (Heck, Schädel, Maretzki, Bartl, & Ritter, 2003). Classical studies (Matthews, Hubbard, Brown, & Wald, 1963; Wald, 1968) suggested that following the hydrolysis of the Schiff base, *tral* separates from the opsin apo-protein. According to this mechanism, subsequent to its release into the ROS cytoplasm, most of *tral* is reduced by *NADPH*-dependent *trans*-retinol dehydrogenase (*tRDH*) to all-*trans* retinol (*trol*) (see Fig. 1a). The remaining *tral* diffuses in the lipid phase where it forms a condensation product with phosphatidylethanolamine. Eventually the condensation product is flipped across the membrane to the ROS cytoplasm by an ATP-binding cassette transporter (ABCR) (Weng, Mata, Azarian, Tzekov, & Birch, 1999) where it is hydrolyzed. *tral* is then reduced by *tRDH* in the cytoplasm.

However, recent studies by Schädel and co-workers (Heck, Schädel, Maretzki, & Hofmann, 2003; Schädel et al., 2003) suggest that a "retinal channeling" mechanism could be the primary pathway of metarhodopsin decay and that the "classical pathway" plays a negligible role in the dynamics of rhodopsin regeneration. According to the channeling hypothesis, following the hydrolysis of the Schiff base, *tral* diffuses out of the active site but is prevented from leaving the protein. Instead, *tral* is transported to another retinoid binding site labeled, the "exit site". The exit site is accessible only to the *tral* that is released from the rhodopsin active site (i.e. free *tral* in the lipid phase cannot bind to this site) (Heck et al., 2003). It is at this site that reduction of *tral* by *tRDH* occurs. The resultant *trol* remains attached to this site until a third retinoid binding site labeled the "entrance site" is occupied by a *cral* molecule (see Figs. 1b and 2a). In a process reminiscent of the classical mechanism, it has been proposed that in conditions where large bleaches of rhodopsin exceed the capacity of *tRDH* to reduce *tral*, *tral* dissociates from the exit site and diffuses into the lipid phase (Heck et al., 2003) where

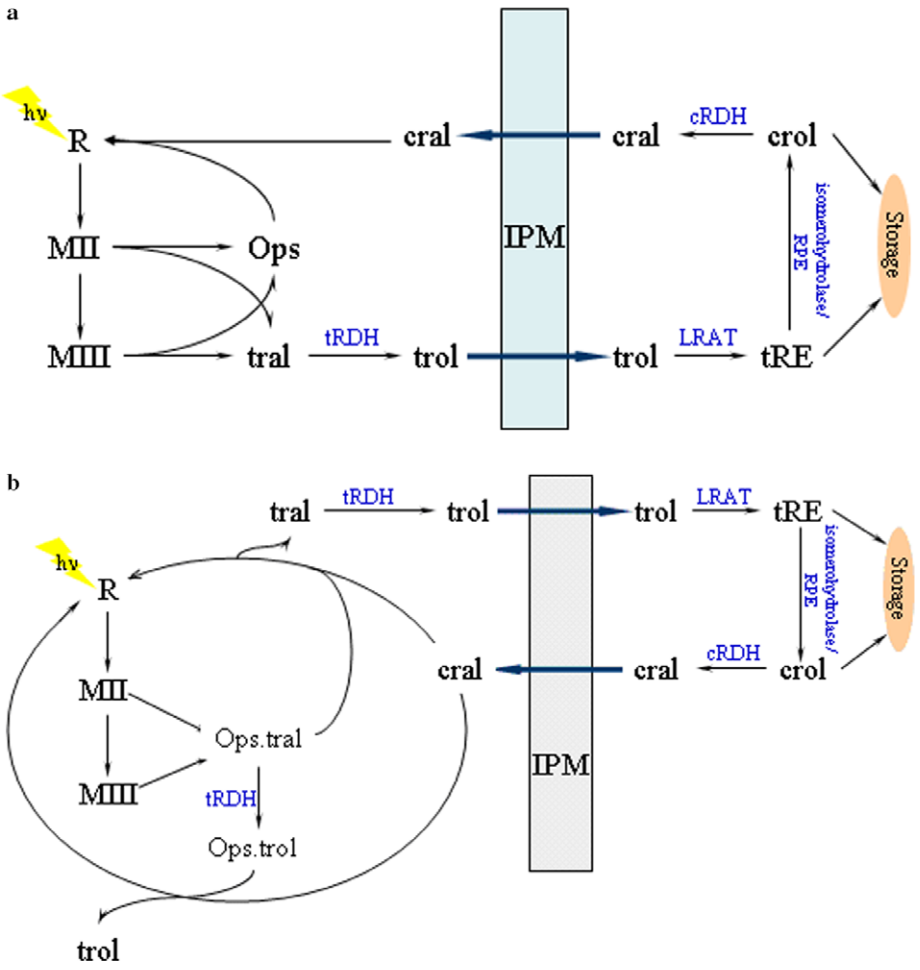

Fig. 1. Retinoid cycle reactions with (a) classical (CLM) and (b) channeling (CHM) mechanism of rhodopsin regeneration (including the reaction proposed by Heck et al., 2003, where *cral* can interact with *Ops · tral* to regenerate a molecule of rhodopsin). For details of the process and definition of abbreviations see the text.

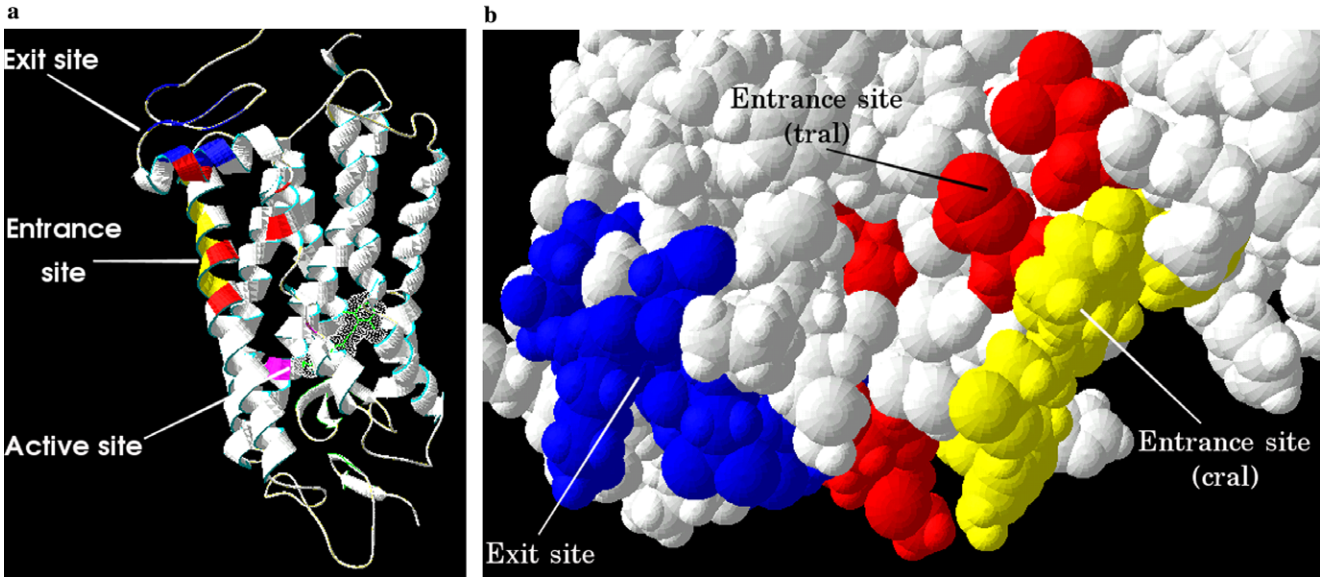

Fig. 2. Proposed retinoid binding sites on rhodopsin. (a) The red colored amino acids of the "entrance site" represent the proposed binding site for *tral*, while the yellow colored amino acids indicate the *cral* binding site (Schädel et al., 2003). The displayed image is that of bovine rhodopsin (pdb 1HZX (Teller et al., 2001)). (b) A closeup look at the location of the retinoid binding sites (Schädel et al., 2003) on bovine metarhodopsin (PDB 1LN6, (Choi et al., 2002)). The yellow colored amino acids indicate the binding site of *cral* at the entrance site, while red amino acids represent the *tral* binding site at the entrance site. The blue colored amino acids denote the retinoid exit site. The location of these three sites are in close enough proximity to each other that it is possible that binding of two retinoids could sterically hinder the binding of a third. Images produced using Deepview/Swiss-pdbViewer.

it eventually is transported back to the cytoplasm via the action of ABCR.

Regardless of the mechanism of metarhodopsin decay, the resultant *trol* is transported across the inter-photoreceptor matrix and into the RPE where, following a series of reactions, it is re-isomerized back to *cral*. Upon *trol*'s entrance into the RPE, fatty acids are used to esterify *trol* in a reaction catalyzed by lecithin:retinol acyltransferase (Berman, Horowitz, Segal, Fisher, & Feeney-Burns, 1980; Rando, 1991; Ruiz, Winston, Lim, Gilbert, & Rando, 1999; Saari & Bredberg, 1988; Saari & Bredberg, 1989; Shi, Furuyoshi, Hubacek, & Rando, 1993; Shi, Hubacek, & Rando, 1993). The resulting all-*trans*-retinyl ester (*tRE*) is then chaperoned by the protein RPE65 to a retinyl ester isomerohydrolase (Gollapalli, Maiti, & Rando, 2003; Gollapalli & Rando, 2003a, 2003b; Mata, Moghrabi, Lee, Bui, & Radu, 2004; Moiseyev, Crouch, Goletz, Oatis, & Redmond, 2003) which catalyzes its conversion to 11-*cis* retinol (*crol*). It should be noted that recent reports have nominated RPE65 as the previously unidentified isomerohydrolase enzyme (Moiseyev, Chen, Takahashi, & Wu, 2005; Moiseyev, Takahashi, Chen, Gentleman, & Redmond, 2006; Redmond, Poliakov, Yu, Tsai, & Lu, 2005). Finally, the cycle is completed when the *crol* is oxidized by 11-*cis* retinol dehydrogenase to *cral* and is transported back to the ROS.

Recently, Mahroo, Lamb and Pugh (MLP), (Lamb & Pugh, 2004; Mahroo & Lamb, 2004) have developed a rate-limited model of pigment regeneration in vertebrate photoreceptors that accounts for various aspects of dark adaptation and for the effects of some genetic mutations that lead to defective retinoid delivery and visual dysfunction (Lamb & Pugh, 2004; Mahroo & Lamb, 2004; Wenzel, Oberhauser, Pugh, Lamb, & Grimm, 2005). However, despite its predictive utility, the MLP model is unable to account for the observation that rhodopsin regeneration has an early fast recovery phase, and a later slow phase (Jäger, Palczewski, & Hofmann, 1996; Kolesnikov, Shukolyukov, Cornwall, & Govardovskii, 2006). We believe that the cause of this shortcoming is that in MLP, the dynamics of metarhodopsin decay are ignored and only the process of recombination of *cral* with opsin and/or the opsin-*trol* complex (*Ops* · *trol*) is explicitly modeled.

Additionally, a possible origin of the observed rhodopsin regeneration behavior is the interplay between the two known pathways of metarhodopsin regeneration, i.e. the classical mechanism (CLM) and the channeling mechanism (CHM). In order to examine the relative roles of CHM and CLM on the overall dynamics of photopigment regeneration in human rods, we developed a model that incorporates both pathways into an MLP-like model of *cral* transport and insertion. The difference between this model and MLP is that, where the latter ignores the time course of metarhodopsin decay and *Ops* · *tral* reduction by *tRDH*, we explicitly accounted for the kinetics of these steps.

The results of our simulations show: (a) neither CLM nor CHM can account for the observed rhodopsin regeneration dynamics; (b) simple linear combinations of the two pathways do not account for the fast-slow, bi-phasic nature of rhodopsin regeneration. Based on these results we propose a possible biochemical scheme that can account for photopigment regeneration dynamics. Our new model assumes that all metarhodopsin decays via CHM but with *tral* acting as an end-product inhibitor of the fast binding

reaction of *cral* to *Ops · tral*. The proposed mechanism involves early post-flash binding of *cral* to *Ops · tral*, a process which due to *tral* inhibition eventually is replaced by *cral* binding to *Ops-trol*. This scheme can accurately account for the data, including the two phases of photopigment regeneration.

2. Models and methodology

Our models builds upon the MLP model of the retinoid cycle. The major differences from the MLP model are:

(a) We include the interconversion of *MII* and *MIII*, and the decay of these species via the classical pathway and/or the channeling mechanism.
(b) We specifically account for the activity of the enzyme all-*trans* retinol dehydrogenase.

Models were developed using *Karyote* cell simulator (Ortoleva, Berry, Brun, Fan, & Fontus, 2003; Weitzke & Ortoleva, 2003). The reactions implemented are presented in Table 1. Table 2, lists the parameters used. The models simulate the interactions between two compartments, one representing 20 rod outer segments and other, a single RPE cell (Lamb & Pugh, 2004).

2.1. Model assumptions

1. All the reactions are considered to be finite rate reactions. Thus, the conservation of mass equation for species i in compartment α is written as:

$$\frac{dc_i^\alpha}{dt} = \sum_{\beta \neq \alpha}^{n_c} F_i^{\beta \to \alpha} + \xi_i^\alpha \tag{1}$$

where c_i^α is the concentration of species i in compartment α, n_c is the total number of compartments, $F_i^{\beta\to\alpha}$ is the flux of species i from compartment β into compartment α, and ξ_i^α is the net rate of reactions involving species i.
2. We assume that conversion of rhodopsin to *MII* is instantaneous and that all of our metarhodopsin decay processes are irreversible. The parameters we use for these processes are those reported by Lamb and Pugh (2004) (see Table 2).

Table 1
List of retinoid cycle reactions implemented

	Reaction	Description
1	$MII \underset{k_{MII\to MIII}/Q_{MII\to MIII}}{\overset{k_{MII\to MIII}}{\rightleftharpoons}} MIII$	Metarhodopsin interconversion
Purely channeling mechanism		
2	$MII \xrightarrow{k_{MII}^{CHM}} Ops \cdot tral$	Metarhodopsin decay
3	$MIII \xrightarrow{k_{MIII}^{CHM}} Ops \cdot tral$	Metarhodopsin decay
4	$Ops \cdot tral \underset{k_{tRDH}/Q_{tRDH}}{\overset{k_{tRDH}}{\rightleftharpoons}} Ops \cdot trol$	*tRDH* catalyzed reduction
5	$Ops \cdot trol + cral \xrightarrow{k_R} R + trol$	Bimolecular rhodopsin regeneration
6	$Ops \cdot tral + cral \xrightarrow{k_R} R + tral$	Bimolecular rhodopsin regeneration (Heck's proposal)
Purely classical mechanism		
7	$MII \xrightarrow{k_{MII}^{CLM}} Ops + tral$	Metarhodopsin decay
8	$MIII \xrightarrow{k_{MIII}^{CLM}} Ops + tral$	Metarhodopsin decay
9	$Ops + cral \xrightarrow{k_R} R$	Bimolecular rhodopsin regeneration
10	$tral \underset{k_{tRDH}/Q_{tRDH}}{\overset{k_{tRDH}}{\rightleftharpoons}} trol$	*tRDH* catalyzed reduction
11	$Ops + tral \xrightarrow{k_{tral}} tral \cdot Opsin$	Production of pseudo photoproduct *tral- opsin*
12	$tral - Opsin + cral \xrightarrow{k_R} R + tral$	Bimolecular rhodopsin regeneration
Tral regulation reactions (purely CHM)		
13	$MII + tral \xrightarrow{k_{tral}} MII \cdot tral$	*tral* regulation of metarhodopsin decay
14	$MIII + tral \xrightarrow{k_{tral}} MIII \cdot tral$	*tral* regulation of metarhodopsin decay
15	$MII \cdot tral \underset{k_{MII\to MIII}/Q_{MII\to MIII}}{\overset{k_{MII\to MIII}}{\rightleftharpoons}} MIII \cdot tral$	Metarhodopsin interconversion
16	$MII \cdot tral \xrightarrow{k_{MII}^{CHM}} Opscdot2tral$	Metarhodopsin decay
17	$MIII \cdot tral \xrightarrow{k_{MIII}^{CHM}} Ops \cdot 2tral$	Metarhodopsin decay
18	$Ops \cdot tral + tral \xrightarrow{k_{tral}} Ops \cdot 2tral$	*tral* regulation of channeling mechanism
19	$Ops \cdot 2tral \underset{k_{tRDH}/Q_{tRDH}}{\overset{k_{tRDH}}{\rightleftharpoons}} trol \cdot Ops \cdot tral$	*tRDH* catalyzed reduction
20	$trol \cdot Ops \cdot tral + cral \xrightarrow{k_R} R + tral + trol$	Bimolecular rhodopsin regeneration

Table 2
List of parameters*

Parameter	Value				(Equation) or reaction	Source
	Pure CLM	Pure CHM	CHM and CLM	End-product regulation		
V^{ROS}	1.812 pL				(4,6,7)	A
A	3.6×10^{-3} mm^2				(4,6,7)	A
n	1×10^{8}					B
$[R]$	$20n/V^{ROS}=2.6$ mM					
K_m	0.52 mM	0.52 mM	0.52 mM	0.39 mM		C
$k_{MII\rightarrow MIII}$	6.67×10^{-5} s^{-1}				1,15	C
$Q_{MII\rightarrow MIII}$	170				1,15	C
k_{tRDH}	2.4 s^{-1}				4,10,19	D[a]
Q_{tRDH}	0.1				4,10,19	E
$[cral]_{RPE}$	0.169 mM					F[a]
k_{MII}	6.16×10^{-3} s^{-1}					C
k_{MIII}	1.05×10^{-2} s^{-1}					C
x_{CLM}	1	0	$0<x_{CLM}<1$	0		
k_{MII}^{CLM}	$x_{CLM}\times k_{MII}$				7	
k_{MIII}^{CLM}	$x_{CLM}\times k_{MIII}$				8	
k_{MII}^{CHM}	$(1-x_{CLM})\times k_{MII}$				2,16	
k_{MIII}^{CHM}	$(1-x_{CLM})\times k_{MIII}$				3,17	
k_R	87 M^{-1} s^{-1}	486 M^{-1} s^{-1}	207 M^{-1} s^{-1}	292 M^{-1} s^{-1}	5,6,9,12,20	C[b]
k_{tral}	$k_R/2.5$				18	G[c]
$h_{cral}^{RPE\rightarrow ROS}$	$(V^{ROS}/A)\times K_m\times k_R$				(4,6,7,8)	C [b]
$h_{trol}^{RPE\rightarrow ROS}$	$h_{cral}^{RPE\rightarrow ROS}$					

A, Hoang et al. (2002); B, Unger et al. (1997); C, Lamb and Pugh (2004); D, Belyaeva et al. (2005); E, Palczewski et al. (1994); F, Maeda et al. (2005); G, Jäger et al. (1996).

[a] Based on observations in prRDH−/− mice that the rate of production of *trol* in these animals was a quarter of that for wild type (Maeda et al., 2005), we multiplied the turnover number reported by Belyaeva et al. by four and used this value in our simulations.

[b] We optimized the $h_{cral}^{RPE\rightarrow ROS}$ and k_R parameters to fit to the experimental data using the range of K_m value from Lamb and Pugh (2004).

[c] k_{tral} was determined by using the optimized k_R value and the experimental observation (Jäger et al., 1996) that for opsin $k_R = 2.5\times k_{tral}$.

* Unless otherwise listed, the values listed under pure CLM were used for all four models.

3. Although the activity of ATP-binding cassette transporters (ABCR) is of utmost importance to the overall health of retina (see Cideciyan, Aleman, Swider, Schwartz, & Steinberg, 2004; Mata, Tzekov, Liu, Weng, & Birch, 2001; Suarez, Biswas, & Biswas, 2002; Sun, Smallwood, & Nathans, 2000; Weng et al., 1999), it has been proposed that the activity of ABCR does not significantly affect the dynamics of recovery from a single bleaching exposure (Lamb & Pugh, 2004). Thus, we do not account for the processes involved in the transport of *tral* from the inside of disc membranes to their cytoplasmic surface.
4. As in the MLP model, we assume that the concentration of *cral* in the RPE is constant. This is equivalent to assuming that there is rapid replenishment of *cral* in the RPE from retinoid stores in RPE and choroid (see Bridges, Alvarez, & Fong, 1982; Imanishi, Batten, Piston, Baehr, & Palczewski, 2004).
5. We assume that, under dark adapted conditions *cral* equilibrates between the RPE and ROS, and there is no net transport across the inter-photoreceptor matrix.

The dark concentration of *cral* was derived from measurements by Maeda et al. (Maeda, Maeda, Imanishi, Kuksa, & Alekseev, 2005). We subtracted their measured value of rhodopsin concentration (468 pmol/eye) from their measured value of total *cral* per mouse eye (529 pmol/eye) to come up with a value of 60.9 pmol of free *cral* per mouse eye. Dividing this amount equally between RPE cells and rod outer segments yields an estimate of 30.45 pmol of *cral* in mouse ROS. Assuming that a rhodopsin concentration of 468 pmol/eye corresponds to 2.6 mM, then 30.45 pmol of *cral* in the ROS corresponds to 0.169 mM.

2.2. Model development

The flux of *cral* from RPE to ROS is governed by the equation:

$$F_{cral}^{RPE\rightarrow ROS} = h_{cral}^{RPE\rightarrow ROS}\frac{A}{V^{ROS}}\left(c_{cral}^{RPE}-c_{cral}^{ROS}\right) \quad (2)$$

where A is the area of membrane between RPE and twenty rod outer segments, V^{ROS} is the volume of twenty rod outer segments, and $h_{cral}^{RPE\rightarrow ROS}$ is the parameter quantifying how fast *cral* can traverse the membrane.

In the MLP model, the rate of bimolecular binding reaction ($\zeta(t)$) between *cral* and *opsin* is expressed as:

$$\zeta(t) = k_R c_{cral}^{ROS} O(t) = \frac{\left(c_{cral}^{RPE}-c_{cral}^{ROS}\right)}{R} \quad (3)$$

where k_R is the bimolecular rate constant for binding of *cral* to *opsin* and/or *Ops · trol*, $O(t)$ represents the transient

concentration of the species that *cral* binds to (i.e. *Opsin* and/or *Ops · trol*) and R is the "resistance" to import of *cral* from RPE to ROS.

If, like MLP, we assume that $\zeta(t) = F_{cral}^{\mathrm{RPE}\rightarrow\mathrm{ROS}}$, then using Eq. (3) we can write MLP's R as:

$$R = \frac{V^{\mathrm{ROS}}}{Ah_{cral}^{\mathrm{RPE}\rightarrow\mathrm{ROS}}} \tag{4}$$

MLP's semi-saturation constant (K_{m}) for *Ops-trol* and/or *opsin*'s rate-limited removal can be written as:

$$K_{\mathrm{m}} = \frac{1}{k_{\mathrm{R}}R} = \frac{Ah_{cral}^{\mathrm{RPE}\rightarrow\mathrm{ROS}}}{k_{\mathrm{R}}V^{\mathrm{ROS}}} \tag{5}$$

Since we assume that a cell's dimensions do not change with time, we can write $A/V^{\mathrm{ROS}} = X$, a constant, and thus:

$$K_{\mathrm{m}} = X\frac{h_{cral}^{\mathrm{RPE}\rightarrow\mathrm{ROS}}}{k_{\mathrm{R}}} \tag{6}$$

Based on Eq. (6), we could derive estimates for the values of the bimolecular rate constant k_{R} and $h_{cral}^{\mathrm{RPE}\rightarrow\mathrm{ROS}}$ by fitting the models to experimental data (e.g. reflection densitometry measurements) (Alpern, 1971; Rushton & Powell, 1972). The value of K_{m} was constrained to 0.52 mM (i.e. 0.2 times the total rhodopsin concentration in ROS, Lamb & Pugh, 2004).

3. Results

3.1. Classical mechanism as the sole pathway of metarhodopsin decay does not account for the data

In order to simulate pigment regeneration via a purely CLM pathway of metarhodopsin decay, the rate constants for the CHM reactions were set to zero (see Table 1). Using experimental data (Alpern, 1971; Rushton & Powell, 1972), we optimized the $k_{\mathrm{R}} = 87\ \mathrm{M}^{-1}\,\mathrm{s}^{-1}$ and $h_{cral}^{\mathrm{RPE}\rightarrow\mathrm{ROS}} = 2.27\times10^{-7}\ \mathrm{dm\,s}^{-1}$ values. Results of these simulations are shown in Fig. 3.

Fig. 3 compares the predictions of the pure CLM model with reflection densitometry measurements of rhodopsin regeneration in the human eye (Alpern, 1971; Rushton & Powell, 1972). The CLM, model even with optimized parameters provides a poor fit to the experimental data. Inclusion of the metarhodopsin decay adds a delay to the time course of recovery (Lamb & Pugh, 2004 calculated this delay to be approximately 0.8 min for a hundred percent bleach). The predicted delay varies with bleach levels and, in fact, increases at lower bleach levels.

The problem caused by this delay cannot be ameliorated by adjusting the kinetic parameters so as to match the data more closely for low bleach levels. Indeed, if we optimize $h_{cral}^{\mathrm{RPE}\rightarrow\mathrm{ROS}}$ and k_{R} (while maintaining K_{m} constant across

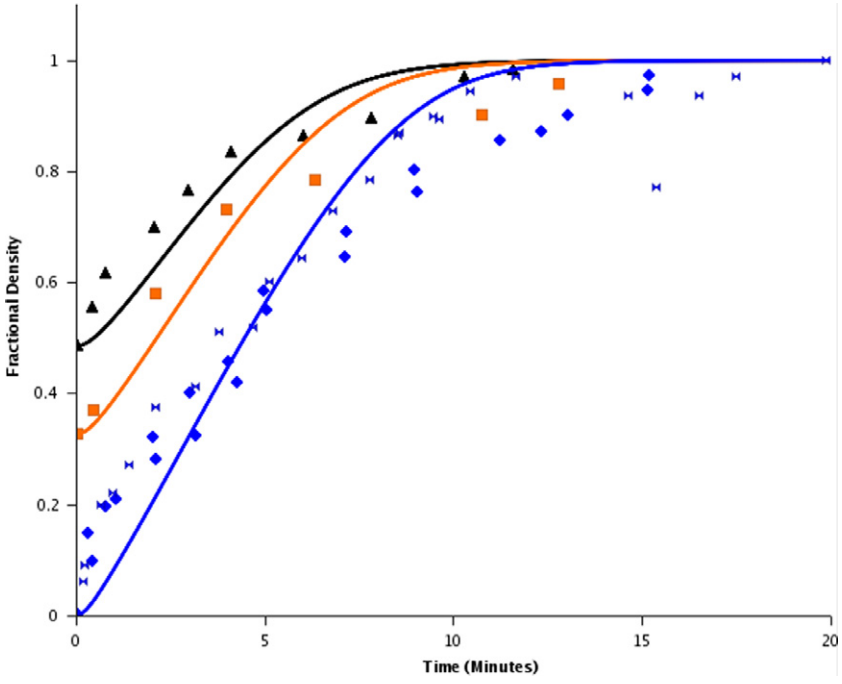

Fig. 3. Rhodopsin regeneration dynamics cannot be accounted for with a model in which CLM is the sole pathway of metarhodopsin decay. The model predictions (solid curves) are compared with reflection densitometry measurements of rhodopsin regeneration in the living human eye (bowties: Alpern, 1971; all other data: Rushton and Powell, 1972). Results for three bleach levels are shown: 51.5% (triangles), 67% (squares), and 100% (bowties and diamonds). Because our implementation of the CLM model includes explicit equations for metarhodopsin decay, as well as for reduction of *tral* to *trol* by *tRDH*, the predicted regeneration dynamics have a sigmoidal shape, and thus do not increase as quickly as the regeneration data. The extent of this delay in rhodopsin regeneration is more pronounced for smaller bleaches.

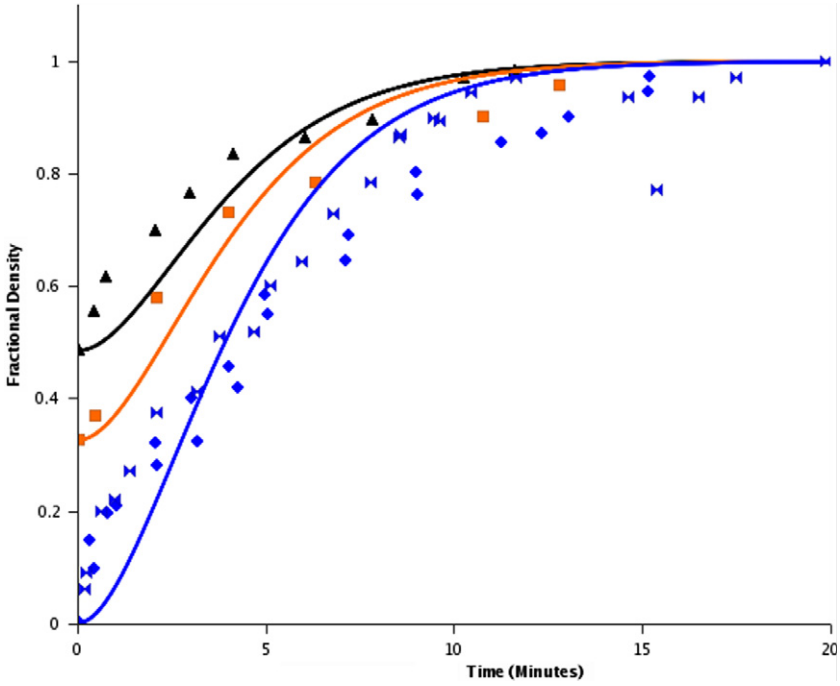

Fig. 4. Rhodopsin regeneration dynamics cannot be accounted for with a model in which CHM, as delineated in Schädel et al. (2003), is the sole pathway of metarhodopsin decay. The predicted regeneration dynamics (solid curves) have an even more pronounced sigmoidal shape than for the pure CLM model (Fig. 3). The resulting delay following a bleach fails to reproduce the empirical regeneration dynamics, and, as for the CLM simulation, becomes more pronounced following less intense bleaches. The coding for the model curves and data are the same as in Fig. 3.

bleach levels) so as to fit the data for small bleaches, then the model predictions will fit the data for high bleach levels even more poorly than shown in Fig. 3.

3.2. Channeling mechanism as the sole pathway of metarhodopsin decay does not accurately account for the data

In order to test how well a pure CHM (Heck et al., 2003; Schädel et al., 2003) model would account for the data, we implemented the generation of *Ops · tral* from metarhodopsin as well as the reduction of *Ops · tral* by *tRDH* to form *Ops · trol*. For these simulations, the kinetic parameters for all the non-channeling reactions were set to zero. Thus for these simulations, there is no free *Ops* or *tral* present and all of the decaying metarhodopsin converts to *Ops · tral*.

The results of our simulations with a pure CHM model are shown in Fig. 4. The values for k_R and $h_{cral}^{RPE\rightarrow ROS}$ that yield the best fit for a pure CHM model are over 5 times larger than they are for a pure CLM model ($k_R = 485.5\ M^{-1}\ s^{-1}$ and $h_{cral}^{RPE\rightarrow ROS} = 1.268\times10^{-6}$ dm s^{-1}). This difference is due to the fact that, in the pure CHM model, rhodopsin regeneration dynamics are dependent on the rate-limited reduction of *tral* to *trol* by the enzyme *tRDH*. When the measured experimental values are used for the generation of *Ops · trol* by *tRDH* (Palczewski, Jäger, Buczylko, Crouch, & Bredberg, 1994), the inclusion of this reaction exaggerates the sigmoidal nature of the photopigment regeneration dynamics as compared with the CLM simulations (see Fig. 3). We can improve the result for small bleaches by increasing k_R and *cral* flux, but this leads to a severe mismatch with the data from more intense bleaches (recovery is far too fast, results not shown).

These simulations show that a model in which metarhodopsin decay proceeds entirely via the proposed CHM (Heck et al., 2003; Schädel et al., 2003) does not provide an accurate account of the dynamics of rhodopsin regeneration, particularly for the first few minutes following the flash.

A special case of the CHM model merits consideration. For scenarios where large bleaches of rhodopsin may exceed the capacity of *tRDH*, regeneration via CHM could proceed through the binding of *cral* to *Ops · tral*, and simultaneous release of a *tral* from the exit site (Heck et al., 2003). The freed *tral* would then diffuse into the lipid phase where it would undergo some changes (see Discussion) and eventually is transported back to the cytoplasm through the action of ABCR. In order to evaluate the effect of this alternate hypothesis on the dynamics of rhodopsin regeneration we added to the CHM model the proposed interaction between *Ops · tral* and *cral* (see Table 1). For these simulations we used the same k_R for binding of *cral* to *Ops · tral* and *Ops · trol*.

The results of these simulations are shown in Fig. 5. They are in closer agreement with experimental data than when *cral* was restricted to bind only to *Ops · trol*. The results, in fact, are similar to those shown in Fig. 3 (pure CLM rhodopsin regeneration). Given the fact that the rate

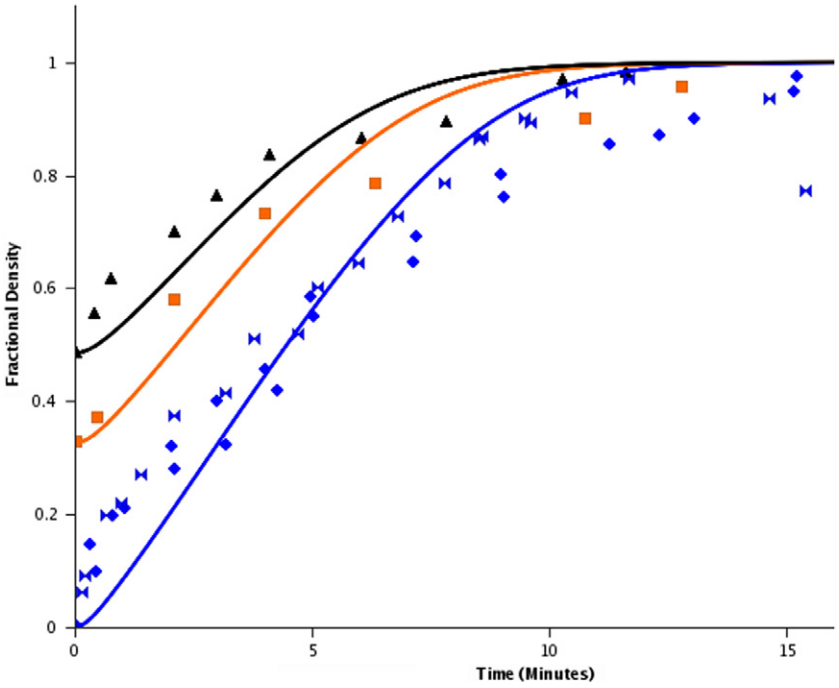

Fig. 5. Simulation of a special case of CHM as the sole pathway of rhodopsin regeneration. If bleaches exceed the capacity of *tRDH*, it has been proposed that regeneration could proceed via CHM through the binding of *cral* to *Ops · tral*, and simultaneous release of a *tral* from the exit site (Heck et al., 2003). Thus, for these simulations we allowed *cral* to bind to *Ops · tral* as well as *Ops · trol* using $k_R = 87\ M^{-1}\ s^{-1}$ for both, and $h_{cral}^{RPE\rightarrow ROS} = 2.27 \times 10^{-7}$ dm s^{-1}. The results are in closer agreement with experimental data than when *cral* was restricted to bind only to *Ops · trol*, as in Fig. 4. The less pronounced sigmoidal dynamics are similar to the predictions from the CLM model. Symbology as in Figs. 3 and 4. (For interpretation of the references to color in this figure legend, the reader is referred to the Web version of this article.)

of formation of *Ops* and *Ops · tral* are equal in the model, similarity is not surprising.

The predicted amount of free *tral* that is produced for these simulations is very high. Our results indicate that over 90% of regenerated rhodopsin is produced via combination of *cral* with *Ops · tral*. Since one of the proposed advantages of CHM is that it protects the ROS from being flooded by toxic *tral*, this scheme, as proposed, seems to invalidate one of the main arguments for the physiological necessity of CHM. Based on this result we can conclude that either: (a) *cral* does not interact with *Ops · tral*, or (b) the rate of combination of *cral* to *Ops · tral* is slower than that of *cral* with *Ops · trol*, or (c) interaction of *cral* with *Ops · tral* is somehow regulated by an end-product. Since there is no physiological basis for the first two hypotheses, we propose that for a purely CHM process, an end-product regulatory mechanism has to govern the dynamics of *cral* binding to different opsin-retinoid complexes.

3.3. Combined metarhodopsin decay via both CLM and CHM does not account for the measured data

Next we simulated conditions where both classical and channeling mechanisms control metarhodopsin decay. Fig. 6 shows the results of two such cases; the combination that gave us the best overall fit to experimental data (57% CLM:43% CHM (a)), and one where the results for low bleaches were relatively improved (80% CLM:20% CHM (b)). The k_R value for both sets of simulations were 206.6 $M^{-1}\ s^{-1}$ and $h_{cral}^{RPE\rightarrow ROS} = 5.4 \times 10^{-7}$ dm s^{-1}.

No combination of CHM and CLM provides an adequate account of the measured early post flash dynamics of rhodopsin regeneration. When CHM dominates, a sigmoidal form is imposed on the model predictions, and it fails to capture any of the experimental data (especially those for lower bleaches). When CLM dominates (thin gray lines) the model is better able to capture the regeneration dynamics for the two smaller bleaches. However, the high bleach data cannot be satisfactorily reproduced.

3.4. A new proposed scheme to account for the data: tral regulated decay of metarhodopsin

Our analyses indicate that neither the classical mechanism (Fig. 3), nor the channeling mechanism (Figs. 4 and 5), nor linear combinations of the two (Fig. 6) can explain the complex dynamics of rhodopsin regeneration. These results, plus other evidence that rhodopsin regeneration cannot be described by a single exponential function (Kolesnikov et al., 2006) and that it has an early fast and later slow phase (Jäger et al., 1996), led us to examine the notion that regulatory product inhibition might explain the multiphasic dynamics of rhodopsin regeneration.

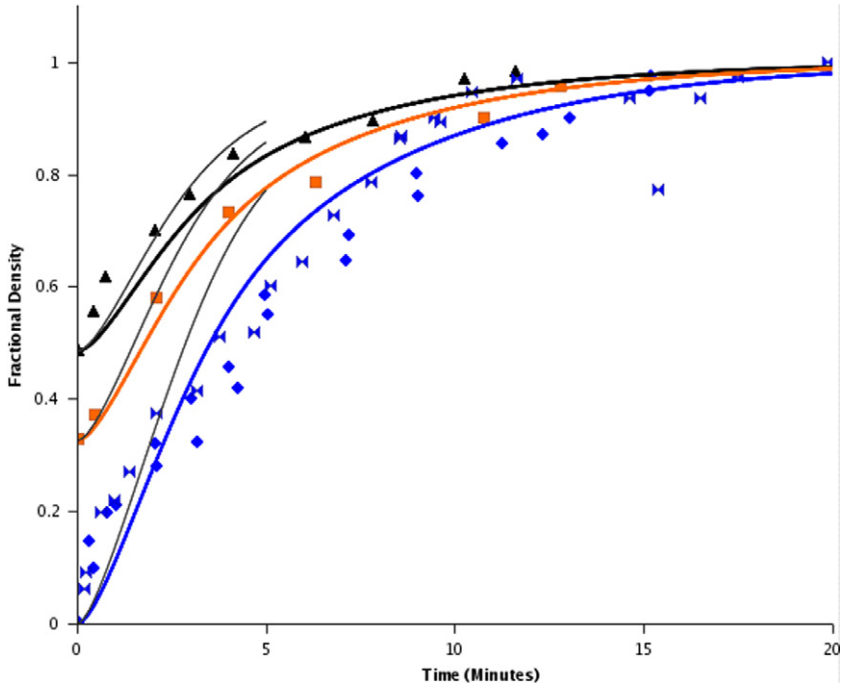

Fig. 6. Predicted dynamics using linear combinations of CHM- and CLM-mediated rhodopsin regeneration are also inadequate to account for the data at all bleach levels. The simulation using the optimal combination of CLM and CHM (57% of the metarhodopsin decay proceeded via CLM, and 43% via CHM), shown as thick solid curves, did not provide an adequate account of the data for all three bleach levels. None of the combinations of CLM and CHM examined were able to account for the multi-phasic regeneration dynamics for all bleach levels. The thin gray curves show the results of a second simulation in which CLM was more dominant in metarhodopsin decay; 80% via CLM and 20% via CHM. This result illustrates our finding that, when both mechanisms are present, greater dominance by CLM provides a better account of the fast, early fast phase of regeneration for all three bleaches. For both simulations $k_R^{CHM} = k_R^{CLM} = 206.6\ M^{-1}\ s^{-1}$. Symbology is the same as in Figs. 3–5. (For interpretation of the references to colour in this figure legend, the reader is referred to the web version of this paper.)

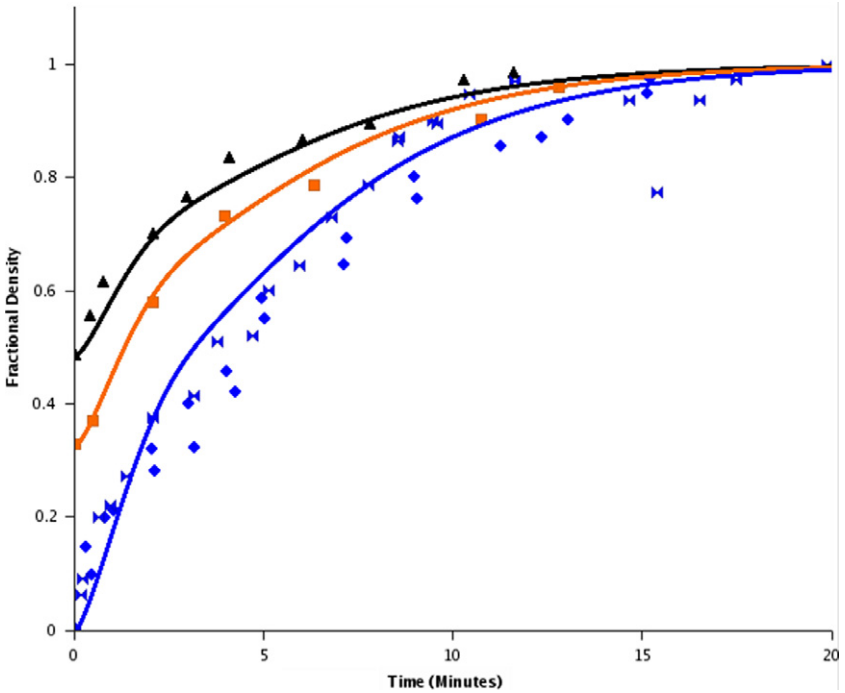

Fig. 7. Our new regulated CHM model can account for the empirical rhodopsin regeneration, including the multi-phasic dynamics, for all three bleach levels using one set of parameters. For these simulations, we implemented a set of regulatory reactions for CHM (see Table 1) whereby binding of *tral* to the *Ops-tral* complex would inhibit its binding to *cral*. The model correctly predicts that the early stages of the regeneration process (the first ~180 s after a bleach) are dominated by the fast binding of *cral* to *Ops-tral* complex. After this fast, early phase, most of the regeneration process then proceeds via binding of *cral* to *Ops-trol*, similar to the unregulated version of the CHM model. Symbology as in Figs. 3–6.

3.4.1. End-product (tral) inhibition of cral binding to Ops · tral

As mentioned in Section 3.2, Heck et al. (2003) have proposed that, following large bleaches of rhodopsin that might exceed the capacity of *tRDH* to reduce *Ops-tral* to *Ops · trol*, rhodopsin regeneration via CHM could proceed through the binding of *cral* to *Ops · tral*. The process leads to simultaneous release of a *tral* from the exit site which then would diffuse into the lipid phase and eventually be transported back to the cytoplasm by the action of ABCR transporter.

Upon examining the location of the proposed retinoid binding sites on rhodopsin (Schädel et al., 2003), we note that the three retinoid binding sites (*tral* at the exit site, *tral* at the entrance site, and *cral* at the entrance site, see Fig. 2b), are clustered in close proximity to one another. Some of the crucial amino acids that form the different binding sites are closely bunched together. Given the proximity of the binding sites, it is possible that binding of retinoids to two of these sites could sterically hinder the binding of retinoids to the third site. For example, if a *trol* is bound to the exit site and a *cral* binds to the entrance site, then the binding of *tral* to the entrance site could be hindered. Based on this assumption, we propose that binding of a *tral* molecule to the entrance site of an *Ops · tral* complex could hinder the binding of *cral* to the entrance site of the same protein. To test whether this type of end-product regulation would allow a purely CHM model to accurately capture the salient features of rhodopsin regeneration dynamics, we implemented such a regulatory scheme (see reactions 13–20 in Table 1). The results of these simulations are shown in Fig. 7.

As can be seen, the results of these simulations closely match the experimental data for all three bleach levels. Furthermore, examination of the amount of *tral* produced by the process shows that, although majority of *cral* interacts with *Ops · tral* molecules, free *tral*'s concentration in the cytoplasm of ROS does not exceed 19% of the total amount of bleached rhodopsin.

4. Discussion

We have developed a new biochemical model of the retinoid cycle in vertebrate rods. An earlier model introduced by Mahroo, Lamb, and Pugh (MLP) (Lamb & Pugh, 2004; Mahroo & Lamb, 2004) was able to account for many of the quantitative details of rhodopsin regeneration across different bleach levels and experimental approaches (reflection densitometry, ERG, psychophysics). However, we sought to explain observed complexities in the rhodopsin regeneration kinetics that were beyond the scope of the MLP model, namely the multi-phasic nature of rhodopsin regeneration that is clearly evident in the reflection densitometry data (see Figs. 3–7). No model to date, including the MLP, predicts the fast early phase and later slow phase evident in these data and noted by others (Jäger et al., 1996; Kolesnikov et al., 2006).

In order to address these problems, we first expanded on the MLP model by including the kinetics of metarhodopsin decay and reduction of *tral* to *trol*. In addition, unlike MLP, we included features of both the classical and channeling mechanisms of metarhodopsin decay.

We found that addition of these explicit kinetic details exacerbated the difficulty in accounting fully for the data (see Figs. 3 and 4). These processes impose an unavoidable sigmoidal rise to pigment regeneration dynamics that is antithetical to capturing the early fast phase of regeneration and the transition into the slow phase. We showed that the two proposed mechanisms for the decay of metarhodopsin and regeneration of rhodopsin, the classical and channeling mechanisms, cannot account fully for the data, either alone (Figs. 3–5) or in combination (Fig. 6).

Experimental observations indicate that pathways analogous to both CLM and CHM contribute to decay of metarhodopsin. The fluorescence spectroscopic data and the results of the molecular modeling simulations presented by Schädel et al., 2003 provide strong support for their proposed channeling mechanism. CHM agrees with Lamb and Pugh's (2004) proposal that the rate limiting step of the retinoid cycle is the delivery of *cral* from RPE to *opsin*/*Ops · trol*. Additionally, the CHM can explain the similarity between the rates of rhodopsin regeneration and release of *trans*-retinoids from the rhodopsin's active site. This is due to the fact that according to the CHM scheme, it is the binding of *cral* to the entrance site of rhodopsin that determines the rate of *trol*/*tral* release into the ROS cytoplasm and not vice versa, as previously had been proposed (Saari, Garwin, & Van Hooser, 1998).

The CHM also makes physiological sense, since it has the fortuitous effect of protecting the system from being flooded by free *tral* which could seriously hinder dark adaptation and lead to a number of retinal diseases. These stated advantages are serious factors that argue against a pure CLM mechanism of metarhodopsin decay. However, it is well known that, as with CLM, some portion of the bleached rhodopsin quickly release their isomerized chromophores into the ROS cytoplasm which eventually reach the lumenal region of the rod discs (Lamb & Pugh, 2004; Weng et al., 1999). Upon release, a portion of this *tral*, through a spontaneous interaction with phophatidylethanolamine, forms the Schiff base *N*-retinylidene-PE (NrPE) (Anderson & Maude, 1970; Beharry, Zhong, & Molday, 2004).

Under normal physiological conditions, NrPE is then removed from the inner region of the disc membrane through the action of the ABCR transporter (Ahn & Molday, 2000; Ahn, Wong, & Molday, 2000; Sun, Molday, & Nathans, 1999; Weng et al., 1999). ABCR is a member of a family of proteins (ATP-binding cassette transporters) that can be found in all species. It uses the energy of ATP hydrolysis to translocate specific chemical species across cellular membranes. The activity of ABCR is crucial to the overall health of the retina and ABCR defects have been shown to lead to a number of retinopathies (Cideci-

yan et al., 2004; Mata et al., 2001; Suarez et al., 2002; Sun et al., 2000). The reason for this is that, in absence of ABCR's "flippase" activity, the NrPE in the rod discs interacts with a second molecule of *tral* to form a phosphatidyl-pyridinium biretinoid species known as A2-PE (Parish, Hashimoto, Nakanishi, Dillon, & Sparrow, 1998) which subsequently forms the compound *N*-retinylidene-*N*-retinylethanolamine (A2E). A2E is the major component of lipofuscin and does not undergo enzymatic degradation. Experiments have shown that alterations of ABCR activity can lead to accumulation of lipofuscin in RPE which eventually leads to a slow demise of the photoreceptors (Cideciyan et al., 2004; Mata et al., 2001; Mata, Weng, & Travis, 2000; Weng et al., 1999).

Despite its clinical importance, it has been proposed that the functioning of ABCR transporter is not of great consequence to the overall processing of retinoids by the retinoid cycle (Lamb & Pugh, 2004). Thus it can be reasoned that under normal conditions, some form of CHM is the primary pathway of metarhodopsin decay.

4.1. Neither CHM nor CLM can act as the sole pathway of metarhodopsin decay

Our theoretical analyses examined whether systems where metarhodopsin decay is purely governed by either CHM or CLM can adequately account for the observed multi-phasic dynamics of rhodopsin regeneration. Figs. 3 and 4 show that neither pathway alone was able to correctly predict the observed regeneration behavior.

4.1.1. Classical mechanism cannot be the only mechanism of metarhodopsin decay

Our CLM simulations confirm the MLP finding that including the time course of metarhodopsin decay in a model imposes a delay, in the calculated dynamics of rhodopsin regeneration in a fully bleached rod (Lamb & Pugh, 2004). Lamb and Pugh argued that this delay is small (approximately 0.8 min) and thus chose not to include metarhodopsin decay in their model. However, our analyses reveal out that the delay associated with formation of opsin increases as the intensity of the bleach decreases, and thus, for smaller bleaches, this delay becomes significant. This greater deviation from the MLP predicted dynamics for smaller bleaches is due to the slower initial rates of metarhodopsin decay for such bleaches.

The initial rate of opsin formation is given by:

$$\frac{\mathrm{d}c_{Ops}(0)}{\mathrm{d}t} = k_{MII}^{\mathrm{CLM}} c_{MII}(0) = k_{MII}^{\mathrm{CLM}} \mathrm{B}[R]_{\mathrm{tot}} \tag{7}$$

where $c_{MII}(0)$ is the concentration of metarhodopsin assumed to be instantaneously formed upon bleaching of rhodopsin; $[R]_{\mathrm{tot}}$ is the pre-flash concentration of rhodopsin in the ROS; and B is the fraction of rhodopsin that was bleached. From this equation we can see that, the initial rate of metarhodopsin decay following 50% bleach would be half of the value for a fully bleached system.

In order to see if we could simulate the multi-phasic dynamics of rhodopsin regeneration by using a purely CLM model, we experimented with varying k_{R} and $h_{cral}^{\mathrm{RPE}\rightarrow\mathrm{ROS}}$ from their optimal values (as shown in Fig. 3), while maintaining MLP's K_{m} constant at 0.52 mM (simulation results not shown). Our aim was to test if it is possible to overcome the delay associated with metarhodopsin decay by expediting the binding of *cral* to *opsin*. We were able to improve the predictions for smaller bleaches by increasing the above values; however this led to excessive increases in the rates of rhodopsin regeneration following large bleaches. Overall, our results, as well as the reported physiological advantages of CHM, argue that CLM cannot be the sole pathway of metarhodopsin decay.

4.1.2. Channeling mechanism cannot be the only mechanism of metarhodopsin decay

If we assume that CHM is the sole mechanism of metarhodopsin decay, and that *cral* can only bind to *Ops · trol*, then the bimolecular rate constant needed to best fit the observed dynamics of rhodopsin regeneration must be more than 5 times larger than it is for a pure CLM mechanism ($k_{\mathrm{R}}^{\mathrm{CLM}} = 87\ \mathrm{M}^{-1}\ \mathrm{s}^{-1}$ while $k_{\mathrm{R}}^{\mathrm{CHM}} = 485\ \mathrm{M}^{-1}\ \mathrm{s}^{-1}$; see Figs. 3 and 4). Even with a larger k_{R}, the CHM model, as delineated in Schädel et al. (2003), can never achieve an adequate fit to the data. This is because the slow kinetics of metarhodopsin decay and reduction of *tral* to *trol* impose an unavoidable pronounced sigmoidal dynamic to the overall rhodopsin regeneration plot (Fig. 4). As we saw for a pure CLM model, parameter adjustment in order to match the fast phase of regeneration causes the model to miss the slow later phase of regeneration (and vice versa).

It might be argued that if *cral* can bind to *Ops · tral* (as proposed by Heck et al. (2003)), it would counteract the slowing of regeneration dynamics associated with the activity of *tRDH*. Indeed, we show in Fig. 5 that the regeneration dynamics predicted for such a scheme are closer to experimental measurements. If one assumes that the k_{R} for binding of *cral* to *Ops · tral* is the same as it is for *Ops · trol*, then the process of regeneration will be dominated by binding of *cral* to *Ops · tral*. However, this would negate one of the main advantages of the CHM, namely that the opsin protein chaperons the toxic *tral* and regulates the release of retinoids into the ROS cytoplasm. Furthermore, like CLM, this mechanism cannot accurately account for the bi-phasic nature of rhodopsin regeneration. It can only account for the dynamics either at high or low bleach levels but not both. Based on these results, it appears that CHM (as proposed by Heck et al., 2003; Schädel et al., 2003) alone cannot account for all the salient features of the regeneration dynamics.

4.2. Unregulated combinations of CHM and CLM cannot accurately predict the observed behavior

We also evaluated whether a linear combination of CLM and CHM could account for the multi-phasic

dynamics of rhodopsin regeneration. To this end, we simulated a variety of scenarios where the metarhodopsin decay kinetics were partitioned between CLM and CHM.

Fig. 6 shows the result of the combination that gave us the best fit to experimental data (solid curves). As with simulations of CHM and CLM alone, the results of these simulations have a sigmoidal shape and thus do not account for the fast early phase of rhodopsin regeneration.

In our simulations, we could find no linear combination of CHM and CLM that could accurately describe the data. When CHM dominated, the delay associated with decay of metarhodopsin and reduction of *Ops · tral* by *tRDH* could not be overcome. For scenarios where CLM dominated (see Fig. 6, thin gray lines), the model could closely predict the dynamics of regeneration following small bleaches. We attribute this improvement to the faster combination of *cral* to *opsin* in comparison to *Ops · trol*. Unfortunately, the faster dynamics associated with CLM dominance have an adverse effect on the predicted dynamics of regeneration for large bleaches.

4.3. Regulation of rhodopsin regeneration dynamics by tral can explain the observed bi-phasic behavior

Examination of Fig. 6 shows that when CLM dominates the dynamics of metarhodopsin decay, the model not only better captures the data for small bleaches, but also better captures the fast early phase of regeneration for all bleach levels. These observations led us to consider a scenario where, for the first few minutes following a flash, the contribution of fast processes like CLM to the process of regeneration dominates and is progressively inhibited thereafter.

4.3.1. End-product inhibition of cral binding to the Ops · tral complex

Because the CHM model has clear physiological advantages (Schädel et al., 2003), we sought a plausible biochemical scheme that could capture the multi-phasic nature of regeneration using a regulated CHM mechanism. In support of such a mechanism is our demonstration (Fig. 5) that, if *cral* is permitted to bind to *Ops-tral* (Heck et al., 2003), the predicted regeneration dynamics will closely resemble the behavior of CLM.

We reasoned that, due to slow activity of *tRDH*, early in the regeneration process *Ops · trol* would be at low concentration. Under such conditions, *cral* binds to *Ops · tral*. We thus implemented a regulatory mechanism whereby the early portion of the rhodopsin regeneration dynamics is dominated by relatively fast binding of *cral* to *Ops · tral*, and is later replaced by the slower binding of *cral* to *Ops · trol*. In our scheme, *tral* is released following the binding of *cral* to *Ops · tral*. This *tral* then binds to another *Ops · tral* complex, inhibiting binding of *cral* to it. Thus as *tral* concentration builds (later in the regeneration process), the fast binding of *cral* to *Ops · tral* is inhibited.

This new model is able to reproduce the retinal densitometry data, including the multi-phasic regeneration dynamics, for all three bleach levels with one set of parameters (Fig. 7). It should be noted here that, to date two different steps of the retinoid cycle have been proposed as the rate-limiting step of the regeneration process. Lamb and Pugh (2004) have nominated the process of transport of *cral* from RPE to ROS and its binding to opsin as the rate-limiting step, while Palczewski (Palczewski et al., 1994) and Saari (Saari, 2000; Saari et al., 1998) have proposed that the activity of *tRDH* is the rate-limiting step in retinoid cycle (in mice). Our proposal serves as a bridge between these two hypotheses. In our regulated CHM model, the early fast portion of the regeneration results from fast binding of *cral* to *Ops · tral*. Thus, the early rhodopsin regeneration is rate-limited by the rate of transport of *cral* from RPE to ROS (similar to Lamb and Pugh's proposal). However, the slow later phase of regeneration is rate-limited by the action of the enzyme *tRDH* (consistent with Saari and Palczewski's suggestion).

4.3.2. Plausibility of the regulated channeling mechanism

It is known that following its release from opsin, *tral* has the ability to bind to rhodopsin and that the presence of these complexes adversely affect the recovery of the visual sensitivity following a flash (Buczylko, Saari, Crouch, & Palczewski, 1996; Jäger et al., 1996; Melia, Cowan, Angleson, & Wensel, 1997; Surya & Knox, 1998). Schädel (Schädel et al., 2003) proposed a location at the rhodopsin entrance site as the site for binding of exogenous *tral* (see Fig. 2b).

A close examination of the proposed locations of retinoid binding sites on rhodopsin shows that the binding sites of *tral* at the entrance and exit sites, as well as the binding site of *cral* at the entrance site, are close to one another. In fact, some of the residues in the proposed binding sites are immediately adjacent to one another (e.g. Cys^{316}, Thr^{319} of *tral* binding location on the exit site, Ile^{54}, Met^{317}, Val^{318} of *tral* binding area on the entrance site, and Pro^{53} of *cral* binding locale at the entrance site). It is reasonable to suppose that steric hindrance would mitigate against simultaneous binding of three retinoids in such close proximity.

One might argue against our regulatory scheme by noting that some experimental results indicate that, when *tral* binds and activates opsin, it does not inhibit the binding of *cral* to opsin (Däemen, 1978; Sachs, Maretzki, Meyer, & Hofmann, 2000). However, these results are for binding of one *tral* and one *cral* to an apo-protein opsin (i.e. the exit site of opsin does not have a *tral* attached to it), and not the concurrent binding of three retinoids.

We also note that Jäger et al. (1996) have reported that they observed bi-phasic rhodopsin regeneration behavior for binding of *cral* to apo-opsin (i.e. in absence of *tral*). However, in their methods, Jäger et al. noted that to remove *tral* from the solution they used an aldehyde-selective gel chromatographic method. Such a method would

preferentially remove the free *tral* from the solution; however, *tral* bound to the exit site of the opsin (as hypothesized by the channeling mechanism) would not be removed. Thus, we argue that Jäger et al.'s bi-phasic results are not incompatible with our model, since they likely represent combination of *cral* with *Ops · tral* and *Ops · trol* and not apo-opsin.

Finally, sachs et al. (Sachs et al., 2000) have presented *in vitro* data that appears to demonstrate that addition of *tral* to opsin initiates a positive allosteric effect, not an inhibitory effect, on the regeneration of rhodopsin. However, inclusion of such an allosteric activation in a model of rhodopsin regeneration would act so as to exaggerate a sigmoidal aspect to the photopigment regeneration. The Sachs et al. results thus seem to be qualitatively incompatible with the *in vivo* densitometry data which do not manifest any appreciable sigmoidal dynamic (Lamb & Pugh, 2004).

5. Conclusions

We implemented detailed models of the retinoid cycle that expanded on the MLP model. We were able to show that neither of the two proposed mechanisms of rhodopsin regeneration—the channeling and classical mechanisms—can account for the complex dynamics of regeneration for all the bleach levels tested. Nor can the data be accounted for by linear combinations of the two mechanisms.

We propose that the multi-phasic dynamics of rhodopsin regeneration in human rods can be explained through end-product (all-*trans* retinal) inhibition of 11-*cis* retinal binding to the *Ops · tral* complex. Our new regulated CHM scheme has the physiological benefit that it prevents the cytoplasm of the ROS from being flooded by toxic *tral* since it predicts that almost equal amounts of *tral* will be chaperoned by the opsin protein at both the entrance site and exit site.

References

Ahn, J., & Molday, R. S. (2000). Purification and characterization of ABCR from bovine rod outer segments. *Methods in Enzymology, 315*, 864–879.

Ahn, J., Wong, J. T., & Molday, R. S. (2000). The effect of lipid environment and retinoids on the ATPase activity of ABCR, the photoreceptor ABC transporter responsible for Stargardt macular dystrophy. *The Journal of Biological Chemistry, 275*(27), 20399–20405.

Alpern, M. (1971). Rhodopsin Kinetics in Human Eye. *The Journal of Physiology, 217*(447-471).

Anderson, R. E., & Maude, M. B. (1970). Phospholipids of bovine outer segments. *Biochemistry, 9*(18), 3624–3628.

Arshavsky, V. Y. (2002). Rhodopsin phosphorylation: from terminating single photon responses to photoreceptor dark adaptation. *Trends Neurosciences, 25*(3), 124–126.

Beharry, S., Zhong, M., & Molday, R. S. (2004). *N*-retinylidene-phosphatidylethanolamine is the preferred retinoid substrate for the photoreceptor-specific ABC transporter ABCA4 (ABCR). *The Journal of Biological Chemistry, 279*(52), 53972–53979.

Belyaeva, O. V., Korkina, O. V., Stetsenko, A. V., Kim, T., Nelson, P. S., et al. (2005). Biochemical properties of purified human retinol dehydrogenase 12 (RDH12): catalytic efficiency toward retinoids and C9 aldehydes and effects of cellular retinol-binding protein type I (CRBPI) and cellular retinaldehyde-binding protein (CRALBP) on the oxidation and reduction of retinoids. *Biochemistry, 44*(18), 7035–7047.

Berman, E. R., Horowitz, J., Segal, N., Fisher, S., & Feeney-Burns, L. (1980). Enzymatic esterification of vitamin A in the pigment epithelium of bovine retina. *Biochimica et Biophysica Acta, 630*(1), 36–46.

Bifone, A., de Groot, H. J. M., & Buda, F. (1997). Ab initio molecular dynamics of rhodopsin. *Pure and Applied Chemistry, 69*(10), 2105–2110.

Bridges, C. D., Alvarez, R. A., & Fong, S. L. (1982). Vitamin A in human eyes: amount, distribution, and composition. *Invest Ophthalmology & Visual Science, 22*(6), 706–714.

Buczylko, J., Saari, J. C., Crouch, R. K., & Palczewski, K. (1996). Mechanisms of opsin activation. *The Journal of Biological Chemistry, 271*(34), 20621–20630.

Burns, M. E., & Arshavsky, V. Y. (2005). Beyond counting photons: trials and trends in vertebrate visual transduction. *Neuron, 48*(3), 387–401.

Burns, M. E., & Lamb, T. D. (2003). 16. Visual Transduction by Rod and Cone Photoreceptors. In L. M. Chalupa & L. S. Werner (Eds.), *The visual neuroscience* (pp. 215–233). MIT.

Burns, M. E., & Taylor, D. A. (2001). Activation, deactivation, and adaptation in vertebrate photoreceptor cells. *Annual Review of Neuroscience, 24*, 779–805.

Choi, G., Landin, J., Galan, J. F., Birge, R. R., Albert, A. D., et al. (2002). Structural studies of metarhodopsin II, the activated form of the G-protein coupled receptor, rhodopsin. *Biochemistry, 41*(23), 7318–7324.

Cideciyan, A. V., Aleman, T. S., Swider, M., Schwartz, S. B., Steinberg, J. D., et al. (2004). Mutations in ABCA4 result in accumulation of lipofuscin before slowing of the retinoid cycle: a reappraisal of the human disease sequence. *Human Molecular Genetics, 13*(5), 525–534.

Däemen, F. J. (1978). The chromophore binding space of opsin. *Nature, 276*(5690), 847–848.

Gollapalli, D. R., Maiti, P., & Rando, R. R. (2003). RPE65 operates in the vertebrate visual cycle by stereospecifically binding all-trans-retinyl esters. *Biochemistry, 42*(40), 11824–11830.

Gollapalli, D. R., & Rando, R. R. (2003a). All-trans-retinyl esters are the substrates for isomerization in the vertebrate visual cycle. *Biochemistry, 42*(19), 5809–5818.

Gollapalli, D. R., & Rando, R. R. (2003b). Specific inactivation of isomerohydrolase activity by 11-cis-retinoids. *Biochimica et Biophysica Acta, 1651*(1-2), 93–101.

Heck, M., Schädel, S. A., Maretzki, D., Bartl, F. J., Ritter, E., et al. (2003). Signaling states of rhodopsin. Formation of the storage form, metarhodopsin III, from active metarhodopsin II. *The Journal of Biological Chemistry, 278*(5), 3162–3169.

Heck, M., Schädel, S. A., Maretzki, D., & Hofmann, K. P. (2003). Secondary binding sites of retinoids in opsin: characterization and role in regeneration. *Vision Research, 43*(28), 3003–3010.

Hoang, Q. V., Linsenmeier, R. A., Chung, C. K., & Curcio, C. A. (2002). Photoreceptor inner segments in monkey and human retina: mitochondrial density, optics, and regional variation. *Vision Neurosciences, 19*(4), 395–407.

Imanishi, Y., Batten, M. L., Piston, D. W., Baehr, W., & Palczewski, K. (2004). Noninvasive two-photon imaging reveals retinyl ester storage structures in the eye. *The Journal of Cell Biology, 164*(3), 373–383.

Jäger, S., Palczewski, K., & Hofmann, K. P. (1996). Opsin/all-trans-retinal complex activates transducin by different mechanisms than photolyzed rhodopsin. *Biochemistry, 35*(9), 2901–2908.

Kennedy, M. J., Lee, K. A., Niemi, G. A., Craven, K. B., Garwin, G. G., et al. (2001). Multiple phosphorylation of rhodopsin and the in vivo chemistry underlying rod photoreceptor dark adaptation. *Neuron, 31*(1), 87–101.

Kolesnikov, A. V., Shukolyukov, S. A., Cornwall, M. C., & Govardovskii, V. I. (2006). Recombination reaction of rhodopsin in situ studied by photoconversion of "indicator yellow". *Vision Research, 46*(10), 1665–1675.

Lamb, T. D., & Pugh, E. N. Jr., (2004). Dark adaptation and the retinoid cycle of vision. *Progress in Retinal Eye Research, 23*(3), 307–380.

Maeda, A., Maeda, T., Imanishi, Y., Kuksa, V., Alekseev, A., et al. (2005). Role of photoreceptor-specific retinol dehydrogenase in the retinoid cycle in vivo. *The Journal of Biological Chemistry, 280*(19), 18822–18832.

Mahroo, O. A., & Lamb, T. D. (2004). Recovery of the human photopic electroretinogram after bleaching exposures: estimation of pigment regeneration kinetics. *The Journal of Physiology, 554*(Pt 2), 417–437.

Mata, N. L., Moghrabi, W. N., Lee, J. S., Bui, T. V., Radu, R. A., et al. (2004). Rpe65 is a retinyl ester binding protein that presents insoluble substrate to the isomerase in retinal pigment epithelial cells. *The Journal of Biological Chemistry, 279*(1), 635–643.

Mata, N. L., Tzekov, R. T., Liu, X., Weng, J., Birch, D. G., et al. (2001). Delayed dark-adaptation and lipofuscin accumulation in abcr+/− mice: implications for involvement of ABCR in age-related macular degeneration. *Invest Ophthalmology & Vision Science, 42*(8), 1685–1690.

Mata, N. L., Weng, J., & Travis, G. H. (2000). Biosynthesis of a major lipofuscin fluorophore in mice and humans with ABCR-mediated retinal and macular degeneration. *Proceedings of the National Academy of Science United States of America, 97*(13), 7154–7159.

Matthews, R. G., Hubbard, R., Brown, P. K., & Wald, G. (1963). Tautomeric forms of metarhodopsin. *The Journal of General Physiology, 47*, 215–240.

McBee, J. K., Palczewski, K., Baehr, W., & Pepperberg, D. R. (2001). Confronting complexity: the interlink of phototransduction and retinoid metabolism in the vertebrate retina. *Progress in Retinal Eye Research, 20*(4), 469–529.

Melia, T. J., Jr., Cowan, C. W., Angleson, J. K., & Wensel, T. G. (1997). A comparison of the efficiency of G protein activation by ligand-free and light-activated forms of rhodopsin. *Biophysical Journal, 73*(6), 3182–3191.

Meng, E. C., & Bourne, H. R. (2001). Receptor activation: what does the rhodopsin structure tell us? *Trends Pharmacology Sciences, 22*(11), 587–593.

Moiseyev, G., Chen, Y., Takahashi, Y., Wu, B. X., et al. (2005). RPE65 is the isomerohydrolase in the retinoid visual cycle. *Proceedings of the National Academy Science United States of America, 102*(35), 12413–12418.

Moiseyev, G., Crouch, R. K., Goletz, P., Oatis, J., Jr., Redmond, T. M., et al. (2003). Retinyl esters are the substrate for isomerohydrolase. *Biochemistry, 42*(7), 2229–2238.

Moiseyev, G., Takahashi, Y., Chen, Y., Gentleman, S., Redmond, T. M., et al. (2006). RPE65 is an iron(II)-dependent isomerohydrolase in the retinoid visual cycle. *The Journal of Biological Chemistry, 281*(5), 2835–2840.

Ohguro, H., Van Hooser, J. P., Milam, A. H., et al. (1995). Rhodopsin phosphorylation and dephosphorylation in vivo. *The Journal of Biological Chemistry, 270*(24), 14259–14262.

Ortoleva, P., Berry, E., Brun, Y., Fan, J., Fontus, M., et al. (2003). The Karyote physico-chemical genomic, proteomic, metabolic cell modeling system. *Omics, 7*(3), 269–283.

Palczewski, K., Jäger, S., Buczylko, J., Crouch, R. K., Bredberg, D. L., et al. (1994). Rod outer segment retinol dehydrogenase: substrate specificity and role in phototransduction. *Biochemistry, 33*(46), 13741–13750.

Parish, C. A., Hashimoto, M., Nakanishi, K., Dillon, J., & Sparrow, J. (1998). Isolation and one-step preparation of A2E and iso-A2E, fluorophores from human retinal pigment epithelium. *Proceedings of the National Academy Science United States of America, 95*(25), 14609–14613.

Rando, R. R. (1991). Membrane phospholipids as an energy source in the operation of the visual cycle. *Biochemistry, 30*(3), 595–602.

Rando, R. R. (2001). The biochemistry of the visual cycle. *Chemical Reviews, 101*(7), 1881–1896.

Redmond, T. M., Poliakov, E., Yu, S., Tsai, J. Y., Lu, Z., et al. (2005). Mutation of key residues of RPE65 abolishes its enzymatic role as isomerohydrolase in the visual cycle. *Proceedings of the National Academy Science United States of America, 102*(38), 13658–13663.

Ritter, E., Zimmermann, K., Heck, M., Hofmann, K. P., & Bartl, F. J. (2004). Transition of rhodopsin into the active metarhodopsin II state opens a new light-induced pathway linked to Schiff base isomerization. *The Journal of Biological Chemistry, 279*(46), 48102–48111.

Ruiz, A., Winston, A., Lim, Y. H., Gilbert, B. A., Rando, R. R., et al. (1999). Molecular and biochemical characterization of lecithin retinol acyltransferase. *The Journal of Biological Chemistry, 274*(6), 3834–3841.

Rushton, W. A., & Powell, D. S. (1972). The rhodopsin content and the visual threshold of human rods. *Vision Research, 12*(6), 1073–1081.

Saari, J. C. (2000). Biochemistry of visual pigment regeneration: the Friedenwald lecture. *Invest Ophthalmology & Vision Science, 41*(2), 337–348.

Saari, J. C., & Bredberg, D. L. (1988). CoA- and non-CoA-dependent retinol esterification in retinal pigment epithelium. *The Journal of Biological Chemistry, 263*(17), 8084–8090.

Saari, J. C., & Bredberg, D. L. (1989). Lecithin: retinol acyltransferase in retinal pigment epithelial microsomes. *The Journal of Biological Chemistry, 264*(15), 8636–8640.

Saari, J. C., Garwin, G. G., Van Hooser, J. P., et al. (1998). Reduction of all-trans-retinal limits regeneration of visual pigment in mice. *Vision Research, 38*(10), 1325–1333.

Sachs, K., Maretzki, D., Meyer, C. K., & Hofmann, K. P. (2000). Diffusible ligand all-trans-retinal activates opsin via a palmitoylation-dependent mechanism. *The Journal of Biological Chemistry, 275*(9), 6189–6194.

Schädel, S. A., Heck, M., Maretzki, D., Filipek, S., Teller, D. C., Palczewski, K., et al. (2003). Ligand channeling within a G-protein-coupled receptor. The entry and exit of retinals in native opsin. *The Journal of Biological Chemistry, 278*(27), 24896–24903.

Shi, Y. Q., Furuyoshi, S., Hubacek, I., & Rando, R. R. (1993). Affinity labeling of lecithin retinol acyltransferase. *Biochemistry, 32*(12), 3077–3080.

Shi, Y. Q., Hubacek, I., & Rando, R. R. (1993). Kinetic mechanism of lecithin retinol acyl transferase. *Biochemistry, 32*(5), 1257–1263.

Suarez, T., Biswas, S. B., & Biswas, E. E. (2002). Biochemical defects in retina-specific human ATP binding cassette transporter nucleotide binding domain 1 mutants associated with macular degeneration. *The Journal of Biological Chemistry, 277*(24), 21759–21767.

Sun, H., Molday, R. S., & Nathans, J. (1999). Retinal stimulates ATP hydrolysis by purified and reconstituted ABCR, the photoreceptor-specific ATP-binding cassette transporter responsible for Stargardt disease. *The Journal of Biological Chemistry, 274*(12), 8269–8281.

Sun, H., Smallwood, P. M., & Nathans, J. (2000). Biochemical defects in ABCR protein variants associated with human retinopathies. *Nature Genetics, 26*(2), 242–246.

Surya, A., & Knox, B. E. (1998). Enhancement of opsin activity by all-trans-retinal. *Experimental Eye Research, 66*(5), 599–603.

Teller, D. C., Okada, T., Behnke, C. A., Palczewski, K., & Stenkamp, R. E. (2001). Advances in determination of a high-resolution three-dimensional structure of rhodopsin, a model of G-protein-coupled receptors (GPCRs). *Biochemistry, 40*(26), 7761–7772.

Unger, V. M., Hargrave, P. A., Baldwin, J. M., & Schertler, G. F. (1997). Arrangement of rhodopsin transmembrane alpha-helices. *Nature, 389*(6647), 203–206.

Wald, G. (1968). Molecular basis of visual excitation. *Nature, 219*, 800–807.

Weitzke, E. L., & Ortoleva, P. J. (2003). Simulating cellular dynamics through a coupled transcription, translation, metabolic model. *Computational Biology and Chemistry, 27*(4-5), 469–480.

Weng, J., Mata, N. L., Azarian, S. M., Tzekov, R. T., Birch, D. G., et al. (1999). Insights into the function of Rim protein in photoreceptors and

etiology of Stargardt's disease from the phenotype in abcr knockout mice. *Cell, 98*(1), 13–23.

Wenzel, A., Oberhauser, V., Pugh, E. N., Jr., Lamb, T. D., Grimm, C., et al. (2005). The retinal G protein-coupled receptor (RGR) enhances isomerohydrolase activity independent of light. *The Journal of Biological Chemistry, 280*(33), 29874–29884.

Yamada, A., Yamato, T., Kakitani, T., & Yamamoto, S. (2004). Torsion potential works in rhodopsin. *Photochemistry and Photobiology, 79*(5), 476–486.

Zhang, L., Sports, C. D., Osawa, S., & Weiss, E. R. (1997). Rhodopsin phosphorylation sites and their role in arrestin binding. *The Journal of Biological Chemistry, 272*(23), 14762–14768.